Nuclear Instruments and Methods in Physics Research B 553 (2024) 165400

Contents lists available at ScienceDirect

Nuclear Inst. and Methods in Physics Research, B

journal homepage: www.elsevier.com/locate/nimb

Scandium thermal release from activated ^{nat}Ti and ^{nat}V target materials in mixed particle fields: Investigation of parameters relevant for isotope mass separation

E. Mamis [a,b,*], P. Kalnina [a,b], C. Duchemin [a], L. Lambert [a], N. Conan [a], M. Deschamps [c], A. Dorsival [a], R. Froeschl [a], F. Ogallar Ruiz [a], C. Theis [a], H. Vincke [a], B. Crepieux [a], S. Rothe [a], E. Pajuste [b], T. Stora [a]

[a] European Organization for Nuclear Research (CERN), Esplanade des Particules 1, 1211 Geneva, Switzerland
[b] Institute of Chemical Physics (ICP), University of Latvia, Jelgavas Street 1, LV-1004 Riga, Latvia
[c] CERAP, Rue du Nant d'Avril 150, 1217, Geneva, Switzerland

ARTICLE INFO

Keywords:
Thermal release
Diffusion
Sc radionuclides
^{nat}Ti and ^{nat}V target materials
Mass separation

ABSTRACT

Scandium (Sc) has gained significant interest in nuclear medicine due to its ^{43}Sc, $^{44g/m}$Sc, and ^{47}Sc radioactive isotopes being suitable for cancer diagnostics and therapy, offering a promising avenue for theranostics. Various production methods, including irradiation of enriched or naturally abundant calcium (Ca), titanium (Ti), and vanadium (V) materials with different particle beams, have been investigated to produce ^{43}Sc, $^{44g/m}$Sc, and ^{47}Sc. However, challenges persist in achieving high molar activity and radiochemical purity for medical applications. The physical isotope mass separation technique presents an alternative, obviating the need for enriched target materials by inherently isolating Sc isotopes during the separation process. Despite recent advancements in Sc mass separation at different facilities, efficiency and yield remain sub-optimal for medical dose production. This study aims to systematically investigate the thermal release kinetics of Sc radionuclides from activated natural titanium foils in tantalum (Ta) environments of ISOL (Isotope Separation On-Line) target units. By elucidating the combination of target material structure and temperature conditions, enhanced release parameters were identified. Maximum Sc release from a non-embossed ^{nat}Ti foil samples was achieved at 1200 °C, for embossed ^{nat}Ti foil samples at 1450 °C and for ^{nat}V foil samples at 1600 °C, within an hour of reaching the set temperature. These findings offer insights into optimizing the mass separation process to improve the efficiency in Sc radionuclide production for medical applications.

1. Introduction

Scandium (Sc) is an element of interest in nuclear medicine because of three radioactive isotopes with decay properties suitable for cancer diagnostics and therapy — theranostics [1]. The advantage of Sc radionuclides is their application in "matched pair" radiopharmaceutical production, where the chemical drug structure is identical both for diagnostic and therapeutic agents [2]. ^{43}Sc ($T_{1/2}$ = 3.891(12) h [3]) is a positron (β^+) emitter that holds great potential for immuno-PET (Positron Emission Tomography) and macro-molecular imaging studies, making it valuable for extended PET examinations [4]. ^{44g}Sc ($T_{1/2}$ = 4.042(25) h [3]) is another promising β^+ emitter for PET and has already been translated to successful in-human proof of concept studies conducted in clinical setting [5,6]. ^{47}Sc ($T_{1/2}$ = 3.3492(6) d [3]) is a β^-emitter with a 159.4 keV (68.3%) gamma-ray emission that would be suitable for therapeutic applications and single-photon emission computed tomography (SPECT) imaging [7]. ^{47}Sc shows potential for use in radio-immunotherapy of tumors by being attachable to monoclonal antibodies (MAb) and conjugates [8]. Nevertheless, the supply of these radionuclides is currently limited due to costly enriched target materials, their enrichment, availability and efficient production capabilities, accessible only at nuclear reactors or medium to high energy cyclotron centers.

To produce ^{43}Sc, $^{44g/m}$Sc, and ^{47}Sc, the irradiation of enriched calcium (Ca) and titanium (Ti) or naturally abundant metallic materials, such as natural calcium, (^{nat}Ca), titanium (^{nat}Ti) and vanadium (^{nat}V) has been investigated using neutrons, proton, deuteron and alpha beams [9]. In the context of enriched material, it is crucial

* Corresponding author at: European Organization for Nuclear Research (CERN), Esplanade des Particules 1, 1211 Geneva, Switzerland.
E-mail address: edgars.mamis@cern.ch (E. Mamis).

https://doi.org/10.1016/j.nimb.2024.165400
Received 25 March 2024; Received in revised form 25 April 2024; Accepted 14 May 2024
Available online 23 May 2024

to emphasize that the enrichment levels must be meticulously optimized to mitigate impurities that could compromise the radionuclide purity of the final sample. Although cost-efficient, the irradiation of natural target materials is accompanied by challenges arising from the presence of other naturally occurring isotopes and the involvement of various nuclear reaction pathways. For instance, the direct production of $^{44g/m}$Sc in ^{nat}Ti occurs through various nuclear reactions, including ^{47}Ti(p, α), ^{48}Ti(p,nα), ^{49}Ti(p,2nα), and ^{50}Ti(p,3nα) [10]. At the same time the long-lived ^{46}Sc ($T_{1/2}$ = 83.79 d, E_γ = 889 keV; 1120 keV) is produced via the ^{47}Ti(p,2p), ^{48}Ti(p,2pn), ^{49}Ti(p,2p2n), ^{49}Ti(p, α) and ^{45}Ti(p,2p3n) nuclear reactions [11]. Notably, the reactions with ^{48}Ti are the primary pathways because of its significant prevalence of 73.8% [12] in natural titanium [13]. Various routes to produce the therapeutic ^{47}Sc are documented, such as employing reactors, cyclotrons, or electron linear accelerators. The main nuclear reactions for ^{47}Sc production are ^{47}Ti(n,p), ^{48}Ti(p,2p), and ^{48}Ca(p,2n) and again suggest the necessity to use enriched target materials to obtain sufficient radionuclide yield [14,15]. However, ^{46}Sc and ^{48}Sc co-production cannot be fully avoided. ^{47}Sc can also be produced with ^{nat}V target irradiation with protons (^{50}V, 0.250% and ^{51}V, 99.750%) [16]. Recent study [16] showed that ^{47}Sc can be produced with a nondetectable amount of ^{46}Sc, however, the production yield is severely decreased. The attractiveness of utilizing natural Ti and V target materials is underlined by their cost-effectiveness, widespread availability and achievable yield with a considerable number of medium-energy cyclotrons in Europe and Worldwide. But it also results in the generation of a diverse array of radionuclides, including Ti, Ca, V and long-lived Sc isotopes. Some of these isotopes are unsuitable for nuclear medicine and cannot be removed with chemical post-processing methods [17]. Another method for Sc radionuclide production could be by using inverse kinematics, where heavy ions, such as Mo, Zn, Ti or V could be impinged on light gas targets and the reaction products caught on a catcher foil. It offers a promising alternative method by allowing precise control over reaction parameters, optimizing yields and minimizing unwanted byproducts [18,19]. Although this route allows for more exotic reaction pathways, the final product still could contain long-lived Sc impurities. Furthermore, a more complex cyclotron, ion source and target system with the possible enriched source material is required to maximize medical Sc radionuclide production yield.

An alternative method for the production of high molar activity, radiochemical pure and medically suitable Sc radionuclides involves the development of a mass separation process. With the mass separation technique, the necessity for utilizing an enriched target material is obviated, as the various isotopes of Sc are inherently isolated during the separation process [20]. MEDICIS (MEDical Isotopes Collected from ISOLDE) facility at CERN (European Organization for Nuclear Research) is specifically designed for the production by mass separation of high-purity novel radionuclides for medical applications [21]. The mass separation method is adapted from ISOLDE (Isotope Separator OnLine DEvice) facility, but the isotopes are produced and mass separated in a batch mode [22]. The radionuclides of interest are produced through the irradiation of thick natural targets with 1.4 GeV protons delivered by the CERN Proton Synchrotron Booster (PSB) [23]. This process allows for the efficient production of the targeted radionuclides in clinically relevant activities. CERN-MEDICIS has successfully produced several radiolanthanides, including samarium (Sm), terbium (Tb), thulium (Tm), and actinium (Ac), which have gained significant attention for targeted radionuclide therapy. These elements share a similar therapeutic potential with ^{177}Lu, a lanthanide already in use in clinical applications [24,25]. Recently at MEDICIS, the medical Sc radionuclides have been produced and mass-separated from irradiated cyclotron-compatible ^{nat}Ti and ^{nat}V target materials. Although high molar activity and radiochemical purity were obtained, the mass separation efficiency and yield are still unsatisfactory for medical dose activity production [26]. Due to the refractory Sc properties, high adsorption enthalpy with tantalum (Ta) ISOL (Isotope Separation On-Line) target unit structures, batch mode experiment limitations, and difficulties in extracting Sc radionuclides from the target units, the conditions for Sc radionuclide release dynamics from metallic ^{nat}Ti and ^{nat}V foils within ISOL target units are not yet fully understood. Multiple studies in radionuclide release from irradiated ISOL target units with various target materials during mass separation have been done at ISOLDE before, however, sufficient post-analysis of the target materials after irradiation was not possible due to the high radiological risks and hazards [27–29]. A study of Sc radionuclide release from 5 μm Ti foil also has been performed, but the impact of thicker foils or multiple layers was not investigated [30].

The objective of this study was to systematically investigate the thermal release kinetics of Sc radionuclides from activated ^{nat}Ti metallic foil rolls in a Ta environment and ISOL target units. Specific focus was placed on understanding the impact of target material structure and temperature conditions on radionuclide release. By studying these factors, the project aimed to study the mechanisms governing Sc release during the mass separation process within the ISOL target unit. By advancing the understanding of these mechanisms, the research outcome paves the way for optimized Sc production via mass separation with high separation efficiency and yield. The study was done in similar conditions as routine radionuclide mass separation done at the CERN-MEDICIS facility. An ISOL-type target unit containing a Ta target container was used and subjected to the same heating method and vacuum conditions, reaching temperatures of 1650 °C. Theoretical estimations were done to estimate radionuclide production in target materials and to identify the possible limiting factors during thermal release. A proof of concept for the methodology to study MEDICIS and ISOLDE-produced radionuclide release kinetics and behavior from various target materials and structures is presented. This work also aims to complement radionuclide release studies in case of fire accidents for radiation protection purposes and provide a way to benchmark theoretical codes. Preliminary results for ^{46}Sc and ^{47}Sc release from activated ^{nat}V foils are also presented.

2. Materials and methods

2.1. General overview

The Sc thermal release data have been experimentally obtained by activating target materials at the CERN High energy AcceleRator Mixed field facility (CHARM) facility [31] followed by thermal release and analysis in class A labs. After irradiation, each sample was analyzed by γ spectrometry, allowing for the quantification of each Sc radionuclide activity specific to each sample before and after the release experiment. Within this experimental framework, each irradiated sample was positioned one by one inside an ISOL target container, always at the same position. The samples were uniformly heated at a constant rate, and then maintained at a pre-defined temperature for one hour. Subsequently, the target container was subjected to a cooling phase, and the sample was then extracted to be measured. Dose rate measurements were conducted for each sample before and after the release, aiming at gathering data regarding potential condensation spots in the target container. γ spectroscopy measurements were performed again to measure the residual activity in the sample. By comparing the radionuclide activity before and after release, a percentage of released fraction of the Sc radionuclides detectable in each sample was calculated and compared with the estimated theoretical data.

2.2. Radionuclide estimation with ActiWiz

The ActiWiz software (version: 3.6.12/2023-2507) is a tool developed at CERN that enables swift assessments of the radiological risks associated with diverse materials employed in high energy particle accelerators [32]. For this purpose, ActiWiz employs a proprietary

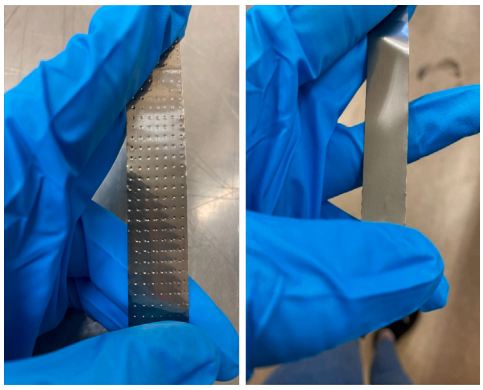

(a) Embossed ^{nat}Ti foil (b) Non-embossed ^{nat}Ti roll

Fig. 1. ^{nat}Ti foils used in roll preparation for thermal release studies and mass separation.

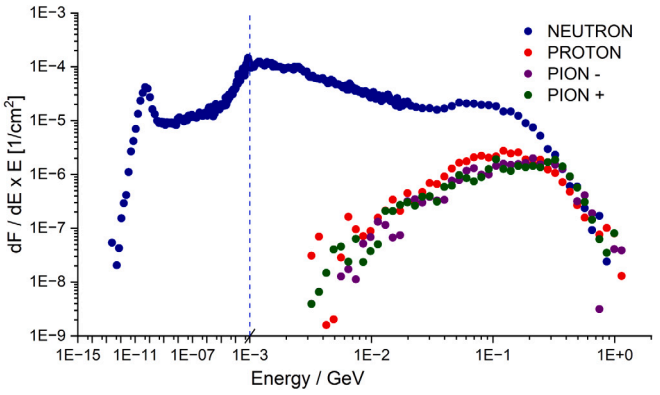

Fig. 2. Fluence spectra (in lethargy representation) at the grid irradiation location of the CHARM facility used to compute the activity values predicted in the Ti samples.

database of isotope production reactions that for neutrons below 20 MeV is based on the evaluated JEFF 3.3 library and for all other reactions utilizes the results of a vast number of FLUKA Monte Carlo simulations [33,34]. It allows for the estimation of nuclide inventories as a function of particle type and energy for user-defined materials using arbitrary particle fluence spectra (neutrons, protons, pions+, pions- and photons) as input. From the results, the users can explore varied compositions and their respective hazards efficiently. ActiWiz has many post-processing options that can be used to analyze the results [35]. The ActiWiz software was used to calculate the total activity and dose rate per sample as well as the targeted activity for each radionuclide of interest according to the CHARM activation scenario.

2.3. Sample preparation

To study Sc thermal release from metallic foils and target material structural impact in MEDICIS mass separation conditions, three different type of samples were prepared : embossed ^{nat}Ti (see Fig. 1(a)), non-embossed ^{nat}Ti (see Fig. 1(b)) and non-embossed ^{nat}V (for preliminary tests and similarly to Fig. 1(b)). The samples were prepared in the form of compact foil (0.25 μm,) rolls with average diameter of 0.46 cm for non embossed samples, 0.80 cm for embossed samples and height 1.5 cm.

For routine mass separation operation, the foils are embossed to reduce the tightness of the sample roll and increase the space between foil layers which reduces the sintering of layers at high temperatures. Therefore the ^{nat}Ti roll sample types differ from one another by their overall volume. Each roll weighs approximately 1 g for ^{nat}Ti and 3.4 g for ^{nat}V samples. The selection of sample weight was based on estimated theoretical radionuclide activity (Bq/g of the sample) according to the irradiation scenarios at CHARM facility and radiation protection aspects.

2.4. Sample activation at the CHARM facility at CERN

The CHARM facility at CERN is dedicated to the study of radiation effects on electronic components and benchmarking various material shielding [36]. The CHARM facility receives a 24 GeV/c proton beam extracted from the CERN proton-synchrotron impinging on a thick copper target. It creates a mixed particle field including secondary neutrons (contribution to the total yield is more than 90%) that were used to activate our samples. A standard 5 day irradiation followed by 1.5 day cooling time after the end of the beam (EOB) with an average proton beam intensity of 5E10 p/s (protons per second) is typically provided by the CHARM facility. This value was first used to estimate the produced activity from Actiwiz calculations. The simulated particle fluence spectra generated by the 5E10 p/s primary proton beam onto the CHARM target is shown in Fig. 2.

Table 1
Average actual proton beam intensity for each irradiation.

Activation run	Average intensity, p/s	Irradiation time, h	Protons on target
I	6.91 E10	132	3.28 E16
II	6.71 E10	126	3.04 E16
III	6.91 E10	139	3.45 E16
IV	6.64 E10	138	3.29 E16

After each activation, the actual average proton beam values and irradiation times were used to estimate more precisely the radionuclide activities (see Table 1). In total four ^{nat}Ti and ^{nat}V target material sample batches were activated at CHARM. In the first activation run only embossed ^{nat}Ti samples were used. In the second activation run non- embossed ^{nat}Ti samples were used. In the third activation run ^{nat}V samples were exposed to the CHARM radiation field, and in the fourth activation run all three types of samples were activated.

2.5. Gamma-ray spectrometry

Gamma-ray spectrometry measurements were performed after the sample activation just before placing each sample inside the target container for release to precisely quantify the radionuclide activities in each sample. The measurements were done with a High Purity Germanium (HPGe) γ-ray detector from MIRION Technologies (Canberra) S.A.S. (energy range from 3 to 10 000 keV with relative efficiency of more than 40%, resolution at 122 keV: $<$ 1.2 keV and at 1332 KeV: $<$ 2.0 keV) [37]. After the Sc release experiments, γ-ray spectrometry measurements were performed again to determine the residual radionuclide activity in the sample and quantify the released Sc radionuclide activity from each sample. The quantitative analysis was performed using the APEX software (V1.4.1) and the ISOCS (In Situ Object Counting System) modelization [38]. For relative measurement purposes, each sample was placed at the same distance from the detector and in the same geometry configuration. Each sample was measured for at least 15 h.

2.6. Thermal release set-up

Isotope mass separation at MEDICIS typically is done at temperatures up to 2300 °C and in vacuum conditions of less than 1E–5 mbar pressure. Often the conditions for release of isotopes are close to the target material melting point [26]. Therefore a specialized ISOL target

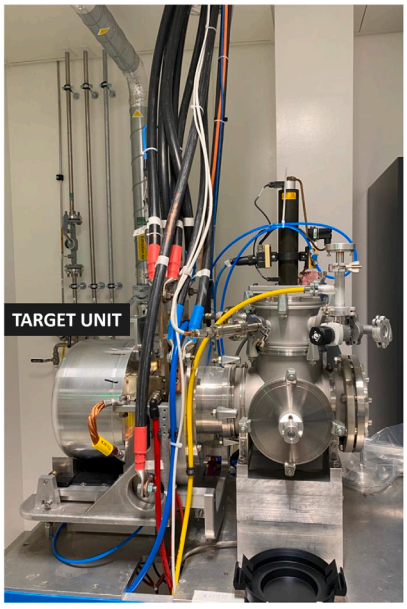

Fig. 3. Set-up for Sc thermal release experiments.

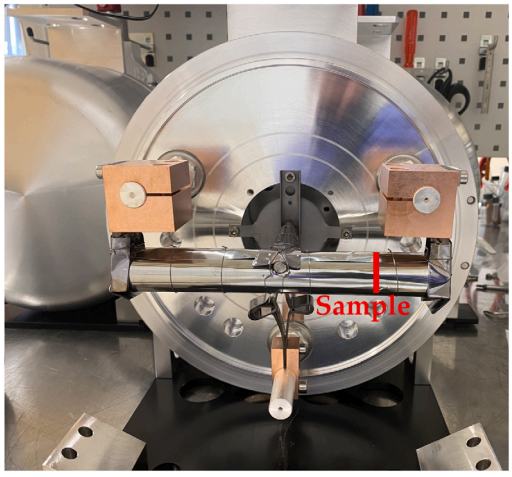

Fig. 4. Opened ISOL target unit back view.

coupling table (pump stand) having the possibility to apply high current (up to 1200 A) for heating and obtain pressure down to 1E–7 mbar was used and is shown in Fig. 3. The pump stand has a dedicated gas exhaust system for any potential radioactive gas trapping.

As the second part of the experimental set-up, a standard ISOL target unit was coupled to the pump stand (see Figs. 3 and 4) [39]. The target unit consists of a target container - Ta tubular oven of 2 cm diameter and 20 cm length - and ion source - hollow Re metallic tube. The target container is perpendicularly connected to the ion source via a transfer line. Since no radioactive ions were needed for this study, the ion source was not heated. The target container and ion source are covered with multiple layers of Ta, W, and Mo heat screens. The target container and ion source are mounted on a water-cooled Al base plate and covered with an Al vessel.

The target is heated by resistive current and the heating ramp by current is correlated to temperature. Five current-regulated (±0.1 A) power supplies were used. Before the experiment, a temperature calibration on the target container was done with a micro-optical pyrometer (see Fig. 5).

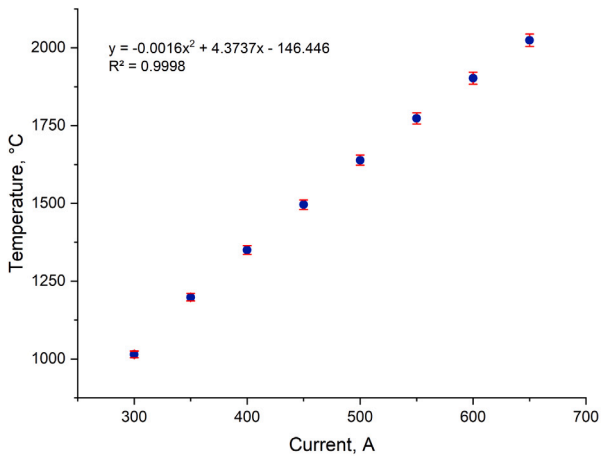

Fig. 5. Target container (oven) temperature calibration curve.

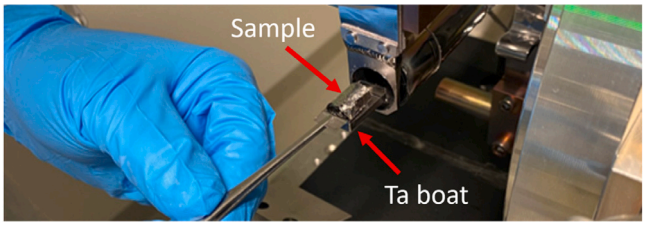

Fig. 6. ^{nat}Ti foil roll sample in a Ta "boat" after thermal release experiment.

2.7. Thermal radionuclide release

To prevent sample fusing with Ta container at high temperatures and allow for a safe and simple exchange of samples from the target container, the samples were placed on a Ta "boat" (see Fig. 6). Once the sample was loaded, the target container was closed with a Ta cap, and the heat screens were mounted. The samples were placed at the same place and distance within the confines of the target container, matching the calibration location (see Fig. 4). The dose rate of the sample and outside the target container with and without the sample was measured before and after the heating phase to determine possible contamination and condensation of the radioisotopes at different places of the target unit structures. Each sample was then subsequently measured by HPGe γ-ray spectrometer (see Section 2.5).

After sample loading, the pressure of the system was stabilized to ≤2E–6 mbar. Once sufficient pressure conditions were reached, each sample underwent a temperature ramp-up process by applying 0.5 A every 25 s to the target container. Once the desired temperature was achieved (as an example to reach 1500 °C it takes 5 h of heating), each sample was maintained at the chosen temperature for one hour and cooled down using the same ramp speed of 0.5 A per 25 s. These initial pressure conditions and heating speed were chosen to allow for target pressure to stabilize and be kept below 1E–5 mbar even during the heating and out-gassing phase. This way also the mass separation conditions were maintained.

2.8. Sc thermal release experimental calculations

The calculation of the relative thermal release of Sc involves the ratio between the activity measured after release and before release, as described in Eq. (1). Decay correction was applied to the initial activity to align with the date and time of the corresponding sample release study.

$$\text{Ratio } R = \frac{A_A}{A_B}, \tag{1}$$

where A_A is the activity measured after sample heating and A_B is the activity measured before performing thermal release experiments with the decay correction. The relative uncertainty related to this ratio is expressed as shown in Eq. (2):

$$\Delta R/R = \sqrt{\left(\frac{\Delta A_A}{A_A}\right)^2 + \left(\frac{\Delta A_B}{A_B}\right)^2} \quad (2)$$

A result reported with 100% release signifies that no activity above the Minimum Detectable Activity (MDA) was measurable. Typically the uncertainty of counting experiments originates from the detection limit (LD) as determined by approaches like the Currie method. However, in the case of gamma spectroscopy the MDA is used as a threshold value which combines the detection limit, calibration efficiency, nuclear data and measurement time [40]. As such it can be considered to be a fundamental characteristic of the measurement itself rather than an uncertainty. It does not directly stem from a single measurement but instead relies on estimations involving uncertainties.

Finally, the release is expressed as Eq. (3), on which the relative uncertainty calculated above is applied:

$$\text{Release} = 1 - \frac{A_A}{A_B} \quad (3)$$

2.9. Thermal release theoretical estimations

The integration of experimental data with modeling allows for a more comprehensive understanding of the release process, which is why complementary calculations have been carried out in this respect.

The release process can be understood as a two-step procedure. For a radionuclide to be released, it must first undergo diffusion within the solid to reach its surface. Subsequently, it must desorb from the surface to escape the solid entirely. To estimate the final release, we have employed the three semi-empirical expressions formulated in [41], based on detailed studies with specifically developed Monte Carlo models. The first of them provides an estimation of the Fraction of Radionuclides reaching the sample's Surface (FRS). This quantifiable parameter is entirely determined by the diffusion stage. The second aims to estimate the so-called Global Desorption Probability (GDP), which quantifies the likelihood of desorption occurring during the remaining heating time for a radionuclide that has successfully reached the surface. The third expression combines the results from the previous two, yielding an estimation of the Out-Diffusion Fraction (ODF), which corresponds to the release fraction integrated over the heating period.

These expressions necessitate user-provided parameters, including heating temperature, heating time, and the surface-to-volume ratio of the sample, which was determined from the foil dimension measurements before preparing the roll. Additionally, users are required to input the relevant diffusion coefficient and desorption activation enthalpy. While experimental data for the former is often accessible, experimental data for the latter is typically unavailable, relying instead on calculated values and, at times, approximations such as sublimation enthalpies [42]. In our study, we have adopted diffusion coefficient parameters from [43] and sourced the desorption activation enthalpy from [44].

3. Results and discussion

Sc thermal release experiments were performed on two different types of ^{nat}Ti foil samples — embossed and non-embossed. Obtained experimental results were compared with the theoretical estimations obtained through the evaluation of the analytical expressions formulated and described by F. Ogallar Ruiz [41]. These calculations give the out-diffused fraction of Sc in ^{nat}Ti for a given sample surface, volume, and temperature. The first Sc release experiments from ^{nat}V samples were performed and a preliminary Sc thermal release curve was obtained.

Table 2
Radionuclides produced in ^{nat}Ti sample.

Radionuclide	Avg. activity per sample (Bq)	MDA interval (Bq)	Half-life ($T_{1/2}$)
^{43}Sc	<MDA	1.41E2–2.02E2	3.89 h
^{44g}Sc	303 ± 56	4.26E1–6.76E1	3.97 h
^{44m}Sc	246 ± 57	4.44E1–6.81E1	2.44 d
^{46}Sc	180 ± 19	2.53E1–4.67E1	83.79 d
^{47}Sc	1730 ± 190	7.57E1–1.02E2	3.35 d
^{48}Sc	496 ± 75	3.19E1–4.67E1	43.67 h

Table 3
Radionuclides produced in ^{nat}V sample.

Radionuclide	Avg. activity per sample (Bq)	MDA interval (Bq)	Half-life ($T_{1/2}$)
^{44g}Sc	53.1 ± 12.4	5.09E1–5.68E1	3.97 h
^{44m}Sc	92.6 ± 21.3	5.24E1–5.44E1	2.44 d
^{46}Sc	59.5 ± 9.5	3.48E1–3.88E1	83.79 d
^{47}Sc	304 ± 54	9.12E1–9.58E1	3.35 d
^{48}Sc	100 ± 14	4.25E1–4.71E1	43.67 h
^{48}V	107 ± 21	4.35E1–4.97E1	15.97 d

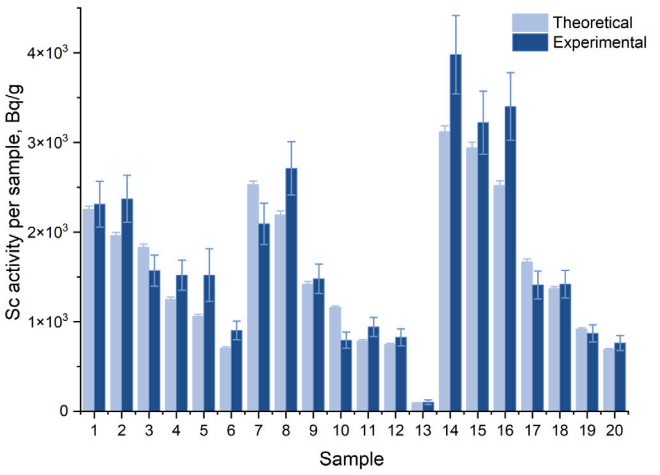

Fig. 7. ^{47}Sc activity per sample given by ActiWiz software versus obtained experimental values with γ-ray spectrometry for ^{nat}Ti samples (the theoretical uncertainties are reported at k = 1).

3.1. Radionuclide production and estimation

The produced Sc radionuclide inventory and the average activity per sample were measured with γ-ray spectrometry and are shown in Tables 2 and 3. $^{44g/m}$Sc, ^{46}Sc, ^{47}Sc and ^{48}Sc radionuclides were produced from which ^{46}Sc and ^{47}Sc were used in the thermal release study because of their favorable decay half-life and relatively higher activity. ^{48}Sc was discarded from the analysis because of the high uncertainties obtained from γ-ray spectrometry measurements due to the short half-life of the radionuclide.

Comparison of theoretical estimations with ActiWiz and experimentally obtained Sc radionuclide activities for neutron activated ^{nat}Ti samples, showcasing the alignment for ^{47}Sc are shown in Fig. 7 and ^{46}Sc in Fig. 8. The average ratio between the obtained values are 1.09 ± 0.13 for the ^{47}Sc and 1.25 ± 0.15 for the ^{46}Sc radionuclides. It is noteworthy that the activity per sample for both ^{47}Sc and ^{46}Sc varies across the samples due to the time gap between irradiation and subsequent γ-ray spectra measurements.

3.2. Sc thermal release from ^{nat}Ti samples

The thermal release of Sc from ^{nat}Ti foil rolls was conducted at various temperatures with a one-hour hold time at the chosen temperature. The selection of temperatures was chosen by the typical mass

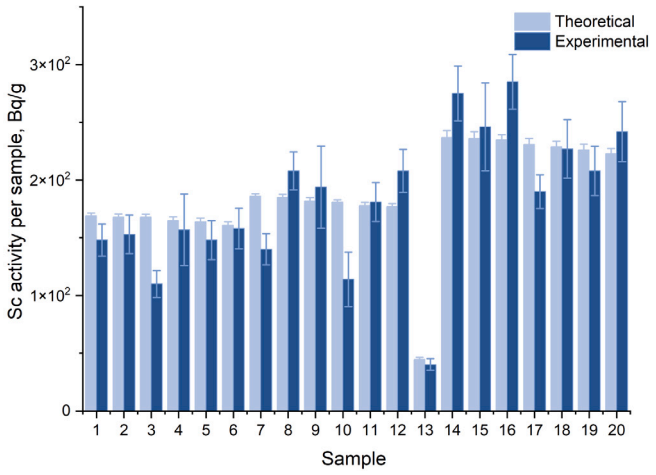

Fig. 8. ^{46}Sc activity per sample given by ActiWiz software versus obtained experimental values with γ-ray spectrometry for ^{nat}Ti samples (the theoretical uncertainties are reported at k = 1).

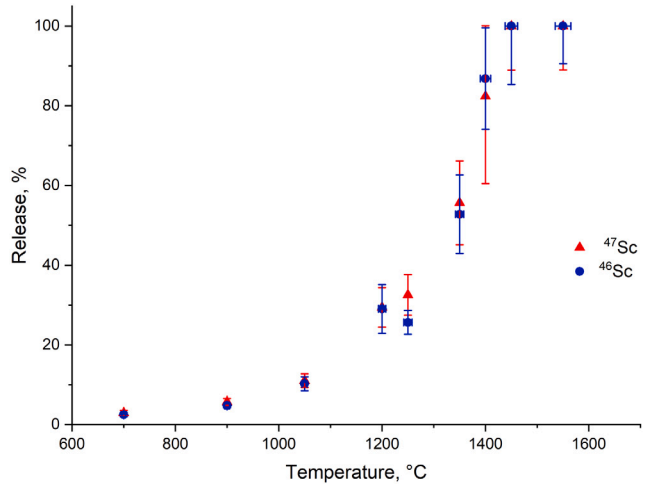

Fig. 9. ^{47}Sc and ^{46}Sc thermal release from embossed ^{nat}Ti foil samples.

separation conditions and physical properties of the material, including considerations such as the melting point. The upper limit was set at 1550 °C to prevent material melting. There was no melting of the material observed for a sample studied at 1500 °C, however, there was a subtle occurrence of sintering, and the sample stuck to the Ta boat. The sintering may be at the source of reduced release over longer periods of operational time during mass separation.

The experimentally obtained relative thermal release results for ^{47}Sc and ^{46}Sc from embossed and non-embossed ^{nat}Ti samples are shown in Figs. 9 and 10. The ^{47}Sc and ^{46}Sc relative release results coincide with each other for both types of roll samples. For both sample types, no release of Sc was observed below 700 °C.

After 1 h at the peak temperature of 1450 °C, 100% scandium release was observed, signifying the complete absence of activity in the sample after the heating cycle. Conversely, for the non-embossed target material, the same release results are shifted to lower temperatures, showcasing the maximum Sc release already at 1200 °C which is in good agreement with previously published studies by [45,46]. It is important to highlight that the uncertainties obtained for samples with longer decay time after the sample activation are notably higher because the activity remaining in the samples closely approached the Minimal Detectable Activity (MDA) values.

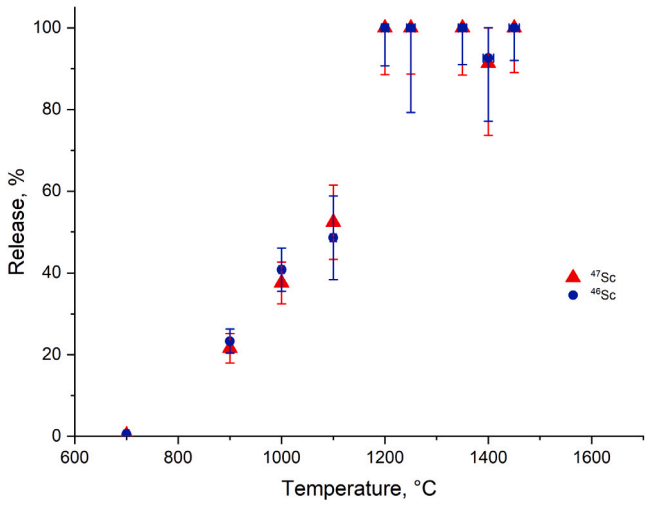

Fig. 10. ^{47}Sc and ^{46}Sc thermal release from non-embossed ^{nat}Ti foil samples.

The observed release shift to the lower temperatures for the non-embossed target material samples compared to its embossed counterpart raises intriguing questions about the impact of surface morphology on thermal release characteristics. This phenomenon could be attributed to several factors. Firstly, the embossing may lead to a slightly larger specific surface area in the embossed material because of the ductile material stretching and compressing. The derived theoretical formulas emphasize the significance of the surface-to-volume ratio in diffusion and release processes. The larger surface area in the embossed material could facilitate greater diffusion potential, theoretically promoting faster release. However, the observed release results in Fig. 9 contradicts this expectation and indicates a delayed release for the embossed material. This suggests, that the actual release kinetics are influenced by a combination of factors beyond the specific surface area. During the sample embossing, possible cracks are being produced at the embossing points on a microscale, which would result in deformation of the crystalline matrix of the native titanium oxide layer that possibly could have a notable impact on the release. The embossing process could also alter the diffusion pathways within the bulk material, affecting the rate at which Sc atoms migrate to the surface and are subsequently released. Also the role of heat conduction could contribute in this context. Better heat conduction implies a more powerful driving force for diffusion, potentially leading to an earlier release. In this scenario, isotopes would likely arrive sooner at the surface, influencing the overall release dynamics. Therefore, the interplay between surface topography, diffusion pathways, and heat conduction should be carefully considered to understand the observed release behavior comprehensively. While larger surfaces generally result in higher release, it is essential to consider the impact of surface effects and chemical compositions on release dynamics. The increased surface area might also increase the interaction between Sc and the surrounding materials and chemical species, explaining the less efficient thermal release. Therefore the additional use of tools and equipment can lead to contaminant deposition into the foil surface, which can stabilize Sc in a less volatile chemical form, such as ScC and Sc_2O_3 [47]. The observed phenomena was not a part of this study and will be further systematically investigated in a future study.

The relative thermal release values of measured Sc radionuclides from both type ^{nat}Ti samples are compiled in Table 4 for embossed ^{nat}Ti and in Table 5 for non-embossed ^{nat}Ti. All uncertainties are presented as combined values derived from both counting statistics (before and after heating). A relative release sum of ^{46}Sc and ^{47}Sc with their according uncertainties at each temperature are shown to highlight the release pattern of Sc species in general.

Table 4
^{46}Sc and ^{47}Sc relative release from embossed ^{nat}Ti foil samples.

Temperature, °C	Release of ^{46}Sc, %	Release of ^{47}Sc, %	Total release of Sc, %
700	2.5 ± 0.5	2.9 ± 0.7	2.7 ± 0.7
900	4.8 ± 0.6	5.7 ± 0.9	5.6 ± 1.0
1050	10.3 ± 1.8	11.0 ± 1.7	10.9 ± 2.9
1200	29.1 ± 6.1	29.4 ± 4.9	29.4 ± 7.4
1250	25.7 ± 3.0	32.6 ± 5.1	31.9 ± 5.8
1350	52.8 ± 9.9	55.6 ± 10.5	54.8 ± 11.0
1400	86.8 ± 12.8	82.3 ± 21.9	83.1 ± 28.0
1450	100.0 ± 14.7	100.0 ± 11.1	100.0 ± 20.4
1550	100.0 ± 9.4	100.0 ± 11.0	100.0 ± 14.5

Table 5
^{46}Sc and ^{47}Sc relative release from non-embossed ^{nat}Ti foil samples.

Temperature, °C	Release of ^{46}Sc, %	Release of ^{47}Sc, %	Total release of Sc, %
700	0.57 ± 0.09	0.33 ± 0.05	0.40 ± 0.08
900	23.3 ± 3.0	21.6 ± 3.6	22.0 ± 4.8
1000	40.8 ± 5.3	37.6 ± 5.1	38.5 ± 5.9
1100	48.6 ± 10.2	52.4 ± 9.1	51.6 ± 10.8
1200	100.0 ± 9.3	100.0 ± 11.4	100.0 ± 15.9
1250	100.0 ± 20.7	100.0 ± 11.3	100.0 ± 18.2
1350	100.0 ± 9.0	100.0 ± 11.6	100.0 ± 13.8
1400	92.6 ± 15.5	91.3 ± 17.7	91.4 ± 18.9
1450	100.0 ± 7.9	100.0 ± 11.0	100.0 ± 24.4

A comparative measurement to assess the heating and cooling ramp influence of the released fraction was also performed for a sample at 1400 °C and changing the hold time from 1 h to 0 h. The measurement was done with a non-embossed ^{nat}Ti foil roll resulting in 51.4 ± 10.6% Sc released. In comparison, the obtained value for the same conditions but with a holding time of 1 h was 91.4 ± 18.9% (see Table 5). Because diffusion and effusion are thermally activated processes, the impact of the heating ramp on the released fraction would be non-linearly higher at higher temperatures not only because of the heating time but also the faster diffusion and desorption. The impact of the heating/cooling ramp time on the released fraction suggests the importance of creating the ion beam and setting the separator for isotope collection already at lower target material temperatures while gradually increasing them throughout the process. Keeping the samples at constant high temperatures would maximize the release [46]. Furthermore, the rapid release may not be suitable for mass separation, because of limited ion source ion load or ionization efficiency. From the obtained results an optimal release plan, target and ion source unit, and mass separation temperatures can be deducted.

To ensure the integrity of the experiment, dose rate measurements on the target container were conducted both with and without the activated samples within the container. This comprehensive approach aimed to monitor and control potential contamination or condensation effects, to identify any cold spots of the target container. The measurements were taken at six distinct points to facilitate a thorough comparison of results before and after the experiment, with Fig. 11 providing an illustrative example of the measurements. Point #4 is the target transfer line which was not heated during the experiments and it remained to stay as a cold spot. During mass separation the ion source and transfer line would be heated to ≈2000 °C and indirectly heat the target container and prevent adsorption in the transfer line region. Point #5 refers to where the sample was placed each time offering a consistent reference point for analysis resulting in a notable difference in dose rate measurements before and after the heating cycle. Points #1 and #6 represent the ends of the container where the temperature is lower than the central region, leading to an increased chance of condensation. It can be seen that a certain amount of released radionuclides migrate towards the ends of the target container. The highest absolute count rate is observed at the end, from which the sample exchange is done, because of the removable target plug and local heat screen assembly, suggesting the highest radionuclide condensation.

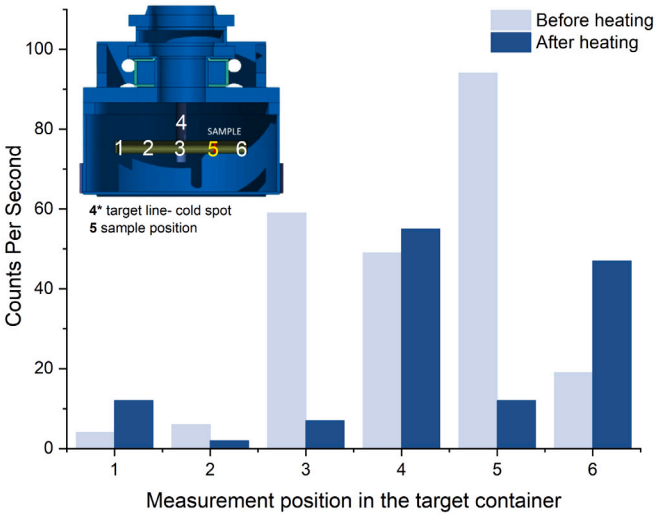

Fig. 11. Target container dose rate measurements in 6 different locations.

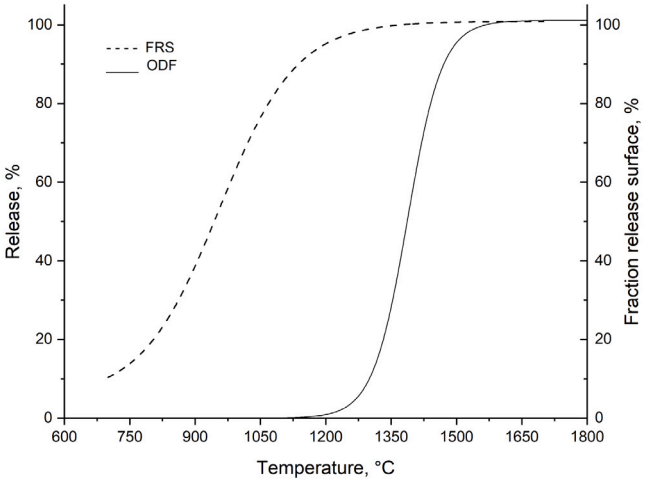

Fig. 12. FRS and ODF theoretical models for Sc thermal release from ^{nat}Ti foil samples.

3.3. Theoretical and experimental result comparison

Comparative analysis using the theoretical models described in Section 2.9 were performed (see Fig. 12) to assess and describe the obtained experimental results, see Fig. 13, by also taking into account the heating ramp speed and release during the heating phase applied during the experiments. While distinguishing between diffusion and surface effects is not the primary goal, accurately modeling the complexities of surface effects, both macroscopic and microscopic, poses a significant difficulty. The theoretical models suggest that radionuclides migrate to the surface much faster than they are released, hinting at surface effects being the limiting factor in the thermal release process. It is noteworthy that the theoretical model did not consider the Ta environment in which the experiments were conducted.

In examining the thermal release curves, our focus centered on the comparison between experimental and theoretical model data. The theoretical estimations indicated a noteworthy trend: radionuclides exhibit a faster migration to the sample's surface than their release rate suggests. This can be understood by the fact that not all isotopes reaching the surface would eventually be released, as there are mechanisms that can retain them and implies that the release process is more constrained by surface effects rather than diffusion itself. It is important to acknowledge that the desorption enthalpy data used in the theoretical model

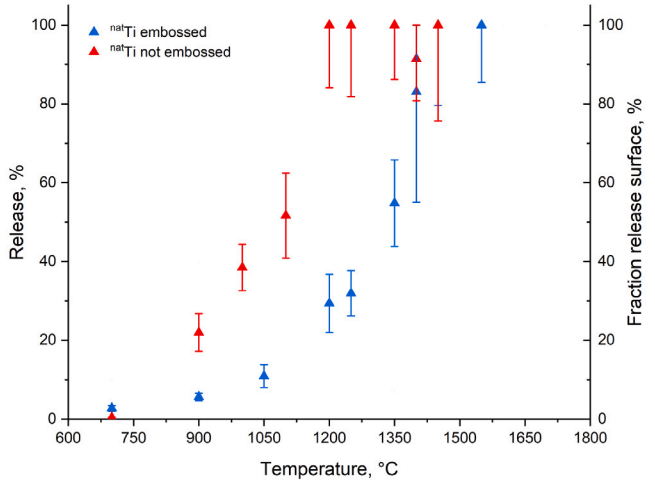

Fig. 13. Total Sc thermal release from embossed and not embossed ^{nat}Ti foil samples.

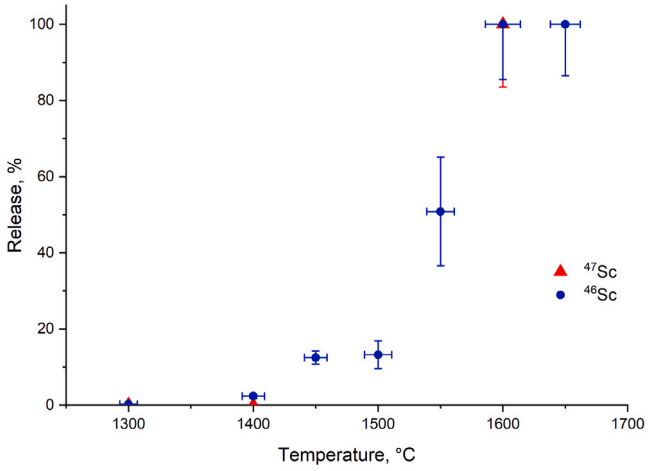

Fig. 14. ^{46}Sc thermal release from non-embossed ^{nat}V foil samples.

is sparsely available in the literature, and its reliability comes with a significant level of uncertainty, which unfortunately is not explicitly documented. This uncertainty may have a substantial impact on the estimation of the global desorption probability and, consequently, on the results obtained for the ODF. Reducing the desorption enthalpy of 392.4 kJ/mol [44] by for example an arbitrary fraction of 5% in the model would shift the onset of the ODF notably towards lower temperatures. Therefore, one cannot draw consistent conclusions from the theoretical model predictions yet with respect to the behavior of embossed and non-embossed samples. It is also important to mention that ^{nat}Ti and ^{nat}V foils are covered with a native oxide layer that can influence the release from the surface because of chemisorption. To better understand these processes further targeted experiments need to be carried out.

3.4. Sc thermal release from ^{nat}V samples

^{nat}V has a higher melting point (1910 °C) than ^{nat}Ti (1668 °C). Moreover, the cross-section (see ref [26]) values for the production of Sc-47 and Sc-44 are in the same order of magnitude for both materials at the energy available at CERN-MEDICIS. Therefore ^{nat}V is a promising material for mass separation and the release of Sc-47 was already investigated at MEDICIS from activated non-embossed ^{nat}V foil samples. The same methodology was used, as described for the ^{nat}Ti samples. The release study temperature points were chosen according to previous mass separation experiments with ^{nat}V foil target materials at MEDICIS [26].

The thermal release results for ^{46}Sc are shown in Fig. 14. Only two data points for ^{47}Sc release results were shown and others were discarded due to the high uncertainties from γ spectroscopy measurements obtained due to the low activity produced. Based on previous mass separation experiments and the fact that V has a higher melting point (1910 °C) and density than Ti (1668 °C), the Sc out-diffusion was expected to happen slower or at higher temperatures [48].

As shown in Fig. 14, there is almost no Sc release below 1450 °C (12.5% ± 1.8%), however, 100% release was observed already at 1600 °C (see Table 6).

Currently, obtaining theoretical estimations and curves for Sc diffusion and release from the ^{nat}V sample is not possible due to the absence of Sc diffusion coefficient data in the ^{nat}V matrix within the literature. However, with a comprehensive understanding of all the processes involved in the Sc thermal release, it would be possible to derive an initial approximation of the diffusion coefficient. The obtained preliminary data serves as a starting point for determining the first diffusion coefficient for Sc within the V matrix.

Table 6
^{46}Sc and ^{47}Sc relative release from non-embossed ^{nat}V foil samples.

Temperature, °C	Release of ^{46}Sc, %	Release of ^{47}Sc, %	Total release of Sc, %
1300	0.27 ± 0.07	0.10 ± 0.03	0.14 ± 0.04
1400	2.4 ± 0.6	0.00 ± 0.23	0.46 ± 0.14
1450	12.5 ± 1.8		
1500	13.2 ± 3.6		
1550	50.8 ± 14.2		
1600	100.0 ± 14.5	100.0 ± 16.5	100.0 ± 23.3
1650	100.0 ± 13.5		

4. Summary and conclusions

The relative Sc radionuclide thermal release pattern from metallic ^{nat}Ti foil and ^{nat}V samples in the MEDICIS and ISOLDE mass separator target unit and Ta environment was systematically studied. Full Sc release within one hour after reaching the set temperature was achieved at 1200 °C for non-embossed ^{nat}Ti, and 1450 °C for embossed ^{nat}Ti foil samples respectively. In contrast to the expected, the Sc radionuclide relative release of embossed metallic ^{nat}Ti foils was shifted towards higher temperatures to achieve the same released fraction. The underlying mechanism of this observation will be investigated in future studies. The first preliminary results for Sc release from ^{nat}V foil samples are presented, showing full (100%) Sc release at 1600 °C within 1 h of reaching the temperature.

The theoretical Actiwiz and mathematical model estimations, used in this study, were in very good agreement with the obtained experimental data for ^{nat}Ti. The obtained preliminary results from experimental Sc release from ^{nat}V foils can serve as a benchmark for theoretical model improvements for V materials.

This study has broader implications, and the methodology and findings of this study not only advance our understanding of Sc release in MEDICIS mass separation conditions but also pave the way for other isotope release studies from ISOL target materials, such as Tb radionuclides from metallic Ta foil target materials as well as build up an experimental database and benchmark theoretical diffusion and release model developments. The starting radionuclide activities in these release experiments, however, should be chosen to maintain them well above the minimal detectable activity levels throughout the whole release experiment, to decrease the uncertainties and therefore increase the experiment output.

CRediT authorship contribution statement

E. Mamis: Writing – review & editing, Writing – original draft, Visualization, Supervision, Methodology, Investigation, Data curation,

Conceptualization. **P. Kalnina:** Writing – review & editing, Writing – original draft, Visualization, Resources, Methodology, Investigation, Formal analysis, Data curation, Conceptualization. **C. Duchemin:** Writing – review & editing, Writing – original draft, Supervision, Project administration, Methodology, Investigation, Formal analysis, Data curation, Conceptualization. **L. Lambert:** Writing – review & editing, Supervision, Investigation, Conceptualization. **N. Conan:** Supervision, Investigation. **M. Deschamps:** Supervision, Investigation. **A. Dorsival:** Supervision, Investigation. **R. Froeschl:** Supervision, Methodology, Investigation, Conceptualization. **F. Ogallar Ruiz:** Writing – review & editing, Writing – original draft, Methodology, Formal analysis, Data curation, Conceptualization. **C. Theis:** Writing – review & editing, Writing – original draft, Methodology, Formal analysis, Data curation, Conceptualization. **H. Vincke:** Writing – review & editing. **B. Crepieux:** Resources, Methodology, Investigation, Conceptualization. **S. Rothe:** Writing – original draft, Supervision, Project administration, Methodology, Investigation, Conceptualization. **E. Pajuste:** Writing – review & editing, Supervision, Funding acquisition, Conceptualization. **T. Stora:** Writing – review & editing, Writing – original draft, Supervision, Resources, Project administration, Methodology, Investigation, Funding acquisition, Conceptualization.

Declaration of competing interest

The authors declare that they have no known competing financial interests or personal relationships that could have appeared to influence the work reported in this paper.

Data availability

Data will be made available on request.

Acknowledgments

This work was supported by the Latvian Council of Science, Latvia, grant number lzp-2021/1-0539 “Novel and efficient approach of medical ^{43}Sc, ^{44}Sc and ^{47}Sc radionuclide separation and purification from irradiated metallic targets towards radiopharmaceutical development for theranostics”, and it has received funding from the European Union’s Horizon 2020 research and innovation program, European Commission under grant agreement No. 101008571 (PRISMAP—the European medical radionuclides programme). This document reflects only the view of the authors. The funding agencies are not responsible for any use that may be made of the information it contains.

The authors extend their gratitude to the CERN-CHARM facility for providing support and the opportunity to activate the samples, enabling the successful execution of this research. Authors express their appreciation to the Radiation Protection Technicians and Coordinators, N. Menaa, D. Bozatto, L. Le, S. Stegemann, and M. Owen.

References

[1] K.P. Carter, G.J.-P. Deblonde, T.D. Lohrey, T.A. Bailey, D.D. An, K.M. Shield, W.W. Lukens Jr., R.J. Abergel, Developing scandium and yttrium coordination chemistry to advance theranostic radiopharmaceuticals, Commun. Chem. 3 (1) (2020) 61.

[2] C. Müller, K.A. Domnanich, C.A. Umbricht, N.P. van der Meulen, Scandium and terbium radionuclides for radiotheranostics: current state of development towards clinical application, Br. J. Radiol. 91 (1091) (2018) 20180074.

[3] Sc medical radionuclide nuclear properties, 2024, https://www.prismap.eu/radionuclides/portfolio/. (Accessed: 2024-4-19).

[4] T.V. Lima, S. Gnesin, K. Strobel, M.d.S. Pérez, J.E. Roos, C. Müller, N.P. van der Meulen, Fifty shades of scandium: Comparative study of pet capabilities using sc-43 and sc-44 with respect to conventional clinical radionuclides, Diagnostics 11 (10) (2021) 1826.

[5] E. Garcia-Torano, V. Peyres, M. Roteta, A. Sanchez-Cabezudo, E. Romero, A.M. Ortega, Standardisation and precise determination of the half-life of 44Sc, Appl. Radiat. Isot. 109 (2016) 314–318.

[6] A. Singh, N.P. van der Meulen, C. Müller, I. Klette, H.R. Kulkarni, A. Türler, R. Schibli, R.P. Baum, First-in-human PET/CT imaging of metastatic neuroendocrine neoplasms with cyclotron-produced 44sc-DOTATOC: a proof-of-concept study, Cancer Biotherapy Radiopharm. 32 (4) (2017) 124–132.

[7] C. Müller, M. Bunka, S. Haller, U. Köster, V. Groehn, P. Bernhardt, N. van der Meulen, A. Türler, R. Schibli, Promising prospects for 44Sc-/47Sc-based theragnostics: application of 47Sc for radionuclide tumor therapy in mice, J. Nucl. Med. 55 (10) (2014) 1658–1664.

[8] L. Deilami-Nezhad, L. Moghaddam-Banaem, M. Sadeghi, M. Asgari, Production and purification of Scandium-47: A potential radioisotope for cancer theranostics, Appl. Radiat. Isot. 118 (2016) 124–130.

[9] A. Jafari, M.R. Aboudzadeh, H. Azizakram, M. Sadeghi, B. Alirezapour, S. Rajabifar, K. Yousefi, Investigations of proton and deuteron induced nuclear reactions on natural and enriched Titanium, Calcium and Vanadium targets, with special reference to the production of 47Sc, Appl. Radiat. Isot. 152 (2019) 145–155.

[10] G. Severin, J. Engle, H. Valdovinos, T. Barnhart, R. Nickles, Cyclotron produced 44gSc from natural calcium, Appl. Radiat. Isot. 70 (8) (2012) 1526–1530.

[11] A. Hermanne, F. Tárkányi, S. Takacs, F. Ditroi, N. Amjed, Excitation functions for production of 46Sc by deuteron and proton beams in natTi: A basis for additional monitor reactions, Nucl. Instrum. Methods Phys. Res. B 338 (2014) 31–41.

[12] S. Takacs, B. Király, F. Tárkányi, A. Hermanne, Evaluated activation cross sections of longer-lived radionuclides produced by deuteron induced reactions on natural titanium, Nucl. Instrum. Methods Phys. Res. B 262 (1) (2007) 7–12.

[13] IAEA, Therapeutic Radiopharmaceuticals Labelled with Copper-67, Rhenium-186 and Scandium-47, IAEA, 2021.

[14] D.A. Rotsch, M.A. Brown, J.A. Nolen, T. Brossard, W.F. Henning, S.D. Chemerisov, R.G. Gromov, J. Greene, Electron linear accelerator production and purification of Scandium-47 from titanium dioxide targets, Appl. Radiat. Isot. 131 (2018) 77–82.

[15] R. Mikolajczak, S. Huclier-Markai, C. Alliot, F. Haddad, D. Szikra, V. Forgacs, P. Garnuszek, Production of scandium radionuclides for theranostic applications: towards standardization of quality requirements, EJNMMI Radiopharm. Chem. 6 (1) (2021) 1–40.

[16] G. Pupillo, L. Mou, A. Boschi, S. Calzaferri, L. Canton, S. Cisternino, L. De Dominicis, A. Duatti, A. Fontana, F. Haddad, et al., Production of 47Sc with natural vanadium targets: results of the PASTA project, J. Radioanal. Nucl. Chem. 322 (3) (2019) 1711–1718.

[17] M. Shahid, K. Kim, G. Kim, H. Naik, Measurement of excitation functions of residual radionuclides from nat Ti (p, x) reactions up to 44 MeV, J. Radioanal. Nucl. Chem. 318 (2018) 2049–2057.

[18] M.R.D. Rodrigues, J. Mabiala, V.E. Iacob, N. Nica, B. Roeder, G. Tabacaru, K. Wang, J. Romo, D. Scriven, N. Tenpas, et al., Production of 99Mo in inverse kinematics heavy ion reactions, Radiat. Phys. Chem. 212 (2023) 111162.

[19] G. Souliotis, M.R.D. Rodrigues, K. Wang, V. Iacob, N. Nica, B. Roeder, G. Tabacaru, M. Yu, P. Zanotti-Fregonara, A. Bonasera, A novel approach to medical radioisotope production using inverse kinematics: a successful production test of the theranostic radionuclide 67Cu, Appl. Radiat. Isot. 149 (2019) 89–95.

[20] C. Duchemin, E. Chevallay, L. Lambert, S. Rothe, J.P. Ramos, R. Catherall, A. Dorsival, R. Heinke, F. Haddad, T. Cocolios, et al., CERN-MEDICIS: a unique facility for the production of non-conventional radionuclides for the medical research, JACoW IPAC 2020 (CERN-ACC-2021-010) (2021) THVIR13.

[21] Y. Martinez Palenzuela, V. Barozier, E. Chevallay, T.E. Cocolios, C. Duchemin, P. Fernier, M. Huyse, L. Lambert, R. Lopez, S. Marzari, et al., The CERN-MEDICIS isotope separator beamline, Front. Med. 8 (2021) 689281, URL https://doi.org/10.3389/fmed.2021.689281.

[22] R.M.d.S. Augusto, L. Buehler, Z. Lawson, S. Marzari, M. Stachura, T. Stora, C.-M. collaboration, CERN-MEDICIS (medical isotopes collected from ISOLDE): a new facility, Appl. Sci. 4 (2) (2014) 265–281.

[23] A. Brown, Design of the CERN MEDICIS Collection and Sample Extraction System (Ph.D. thesis), Manchester U., 2015.

[24] C. Burkhardt, L. Bühler, D. Viertl, T. Stora, New isotopes for the treatment of pancreatic cancer in collaboration with CERN: a mini review, Front. Med. 8 (2021) 674656.

[25] C. Bernerd, J. Johnson, E. Aubert, M. Au, V. Barozier, A.-P. Bernardes, P. Bertreix, F. Bruchertseifer, R. Catherall, E. Chevallay, et al., Production of innovative radionuclides for medical applications at the CERN-MEDICIS facility, Nucl. Instrum. Methods Phys. Res. B 542 (2023) 137–143.

[26] E. Mamis, C. Duchemin, V. Berlin, C. Bernerd, M. Bovigny, E. Chevallay, B. Crepieux, V.M. Gadelshin, R. Heinke, R.M. Hernandez, J.D. Johnson, P. Kalnina, A. Koliatos, L. Lambert, R.E. Rossel, S. Rothe, J. Thiboud, F. Weber, K. Wendt, R.J. Zabolockis, E.n. Pajuste, T. Stora, Target development towards first production of high-molar- activity 44gSc and 47Sc by mass separation at CERN-MEDICIS, Pharmaceuticals 17 (3) (2024) http://dx.doi.org/10.3390/ph17030390, URL https://www.mdpi.com/1424-8247/17/3/390.

[27] P. Hoff, O. Jonsson, E. Kugler, H. Ravn, Release of nuclear reaction products from refractory compounds, Nucl. Instrum. Methods Phys. Res. 221 (2) (1984) 313–329.

[28] T. Bjørnstad, E. Hagebø, P. Hoff, O. Jonsson, E. Kugler, H. Ravn, S. Sundell, B. Vosicki, I. collaboration, et al., Methods for production of intense beams of unstable nuclei: new developments at ISOLDE, Phys. Scr. 34 (6A) (1986) 578.

[29] J. Ramos, Thick solid targets for the production and online release of radioisotopes: The importance of the material characteristics–A review, Nucl. Instrum. Methods Phys. Res. B 463 (2020) 201–210.
[30] D. Wittwer, R. Dressler, R. Eichler, H.W. Gäggeler, D. Piguet, A. Serov, A. Türler, A. Vögele, The thermal release of scandium from titanium metal – a simple way to produce pure 44Sc for PET application, Radiochim. Acta 99 (3) (2011) 193–196, http://dx.doi.org/10.1524/ract.2011.1832.
[31] A. Toscani, D. Santoro, N. Delmonte, P. Cova, C. Concari, A. Lanza, CHARM facility remotely controlled platform at CERN: A new fault-tolerant redundant architecture, Microelectr. Reliab. 115 (2020) 113950.
[32] H. Vincke, C. Theis, ActiWiz – optimizing your nuclide inventory at proton accelerators with a computer code, Prog. Nucl. Sci. Tech. 4 (2014) 228–232, http://dx.doi.org/10.15669/pnst.4.228, URL https://cds.cern.ch/record/2198354.
[33] C. Ahdida, D. Bozzato, D. Calzolari, F. Cerutti, N. Charitonidis, A. Cimmino, A. Coronetti, G. D'Alessandro, A. Donadon Servelle, L. Esposito, et al., New capabilities of the FLUKA multi-purpose code, Front. Phys. 9 (2022) 788253.
[34] G. Battistoni, T. Boehlen, F. Cerutti, P.W. Chin, L.S. Esposito, A. Fasso, A. Ferrari, A. Lechner, A. Empl, A. Mairani, et al., Overview of the FLUKA code, Ann. Nucl. Energy 82 (2015) 10–18.
[35] C. Theis, H. Vincke, The use of ActiWiz in operational radiation protection, in: Proceedings of the Twelfth Meeting of Task-Force on Shielding Aspects of Accelerators, Targets and Irradiation Facilities of Accelerator Technology, SATIF12 FNAL, 2014, pp. 28–30.
[36] R. Froeschl, M. Brugger, S. Roesler, The CERN high energy accelerator mixed field (CHARM) facility in the CERN PS east experimental area, in: Proceedings, 12th Meeting of Task-Force on Shielding Aspects of Accelerators, Targets and Irradiation Facilities, 2015, pp. 14–25.
[37] MIRION spectroscopy and scientific analysis systems, 2023, https://www.mirion.com/products/technologies. (Accessed: 2023-11-30).
[38] C. Duchemin, F. La Torre, M. Magistris, M. Silari, Activation experiment at the H4IRRAD facility: A comparison between experimental data, FLUKA and ActiWiz predictions after 15 days of cooling time, Nucl. Instrum. Methods Phys. Res. A 986 (2021) 164717.
[39] J. Ballof, Radioactive Molecular Beams at CERN-ISOLDE (Ph.D. thesis), Johannes Gutenberg-Universität Mainz, Germany, 2021, Presented 09 December. URL https://cds.cern.ch/record/2797475.
[40] L.A. Currie, Limits for qualitative detection and quantitative determination. application to radiochemistry, Anal. Chem. 40 (3) (1968) 586–593.
[41] F. Ogallar Ruiz, Evaluation and Criticality Assessment of Radiological Source Terms to Be Used for Fire Risk Studies at Accelerator Facilities (Ph.D. thesis), University of Granada, 2021, Presented 03 Feb 2022. URL https://cds.cern.ch/record/2802879.
[42] B. Eichler, S. Huebener, H. Rossbach, Adsorption of Volatile Metals on Metal Surfaces and the Possibilities of Its Application in Nuclear Chemistry, Tech. rep., Zentralinstitut fuer Kernforschung, Dresden, German Democratic Republic, 1986.
[43] J. Askill, Tracer diffusion of silver and Scandium in β-Titanium, Phys. Status Solidi B Basic Res. 43 (1) (1971) K1–K2.
[44] H. Roßbach, B. Eichler, Adsorption von metallen auf metallische oberflächen und möglichkeiten ihrer nutzung in der kernchemie, Zentralinstitut fuer Kernforschung, Dresden, Ger. Democr. Repub. (1984).
[45] I. Alekseev, A. Antropov, D. Maslennikov, Thermal recovery of 47Sc from irradiated metallic titanium, Radiochemistry 43 (2001) 523–524.
[46] D. Wittwer, R. Dressler, R. Eichler, H. Gäggeler, D. Piguet, A. Serov, A. Türler, A. Vögele, The thermal release of scandium from titanium metal–a simple way to produce pure 44Sc for PET application, Radiochim. acta 99 (3) (2011) 193–196.
[47] K. GSCHNEIDNER, CHAPTER 8 - inorganic compounds, in: C. HOROVITZ, K. GSCHNEIDNER, G. MELSON, D. YOUNGBLOOD, H. SCHOCK (Eds.), Scandium: Its Occurrence, Chemistry Physics, Metallurgy, Biology and Technology, Academic Press, 1975, pp. 152–251, http://dx.doi.org/10.1016/B978-0-12-355850-3.50013-7, URL https://www.sciencedirect.com/science/article/pii/B9780123558503500137.
[48] H. Mehrer, Diffusion in Solids: Fundamentals, Methods, Materials, Diffusion-Controlled Processes, vol. 155, Springer Science & Business Media, 2007.